Haxhiu, Arber; Kyyrä, Jorma; Chan, Ricky; Kanerva, Sami

Improved Variable DC Approach to Minimize Drivetrain Losses in Fuel Cell Marine Power Systems

Published in:
IEEE Transactions on Industry Applications

DOI:
10.1109/TIA.2020.3035337

Published: 01/01/2021

Document Version
Peer-reviewed accepted author manuscript, also known as Final accepted manuscript or Post-print

Please cite the original version:
Haxhiu, A., Kyyrä, J., Chan, R., & Kanerva, S. (2021). Improved Variable DC Approach to Minimize Drivetrain Losses in Fuel Cell Marine Power Systems. *IEEE Transactions on Industry Applications*, *57*(1), 882-893. Article 9247287. https://doi.org/10.1109/TIA.2020.3035337

Improved Variable DC Approach to Minimize Drivetrain Losses in Fuel Cell Marine Power Systems

Arber Haxhiu, *Member, IEEE*, Jorma Kyyrä, *Member, IEEE*, Ricky Chan and Sami Kanerva

***Abstract*— This paper proposes a novel approach for operating hybrid fuel cell and battery power systems in marine vessels. The target of the approach is to reduce energy losses in drivetrain devices. In the proposed approach, the DC bus voltage of the hybrid power system is adjusted according to fuel cell operating points, which enables operation in Freewheel mode, and thus significantly reducing power conversion losses. Feasibility of the proposed approach is verified using a real-time hardware-in-loop simulation setup consisting of pre-validated virtual models and real industrial power converter controllers. The results presented in the work illustrate that the Variable DC Approach enables significant improvements in drivetrain efficiencies, and thus providing significant savings for vessel operators. Additionally, Variable DC Approach is shown to eliminate high frequency current ripple at the fuel cell terminals, which can further improve the efficiency and the lifetime of the fuel cells.**

***Index Terms*— Drivetrain, Efficiency, Fuel Cells, Hybrid, Losses, Marine, Power System Control, Variable DC Voltage.**

I. Introduction

The International Maritime Organization is targeting significant reductions in greenhouse gas emissions (50% by 2050, compared to 2008) for the maritime industry. To avoid potential pollutant penalties, vessel operators are searching for alternative power sources which comply with the ever-tightening emission requirements. Hydrogen fuel cells (FCs) and batteries are considered as one means to achieve zero-emission shipping [1]. However, high cost of FCs and hydrogen has been limiting their adoption in marine vessels. Therefore, optimizing efficiencies of systems powered by FCs is key to improve attractiveness of the FCs and batteries.

FCs and batteries are both DC power sources with characteristics of variable terminal voltage as a function of load. Due to this characteristic, DC/DC converters are usually used to connect the power sources to a common DC bus with a fixed DC voltage. Propulsion motors and other onboard hotel load (i.e., lighting, navigation devices, heating and air conditioning, etc.) are connected to the DC bus through voltage source inverters (VSIs). The fixed DC voltage level is usually designed to enable the VSIs to operate at maximum power. However, some marine vessels typically operate at lower loads than dimensioning or design set points. For example, dynamic positioning vessels, offshore vessels or inland navigation vessels have been known to spend up to 90% of total energy consumption when operating at partial loads, less than 60-70% of full power [2], [3].

In order to reduce losses in power electronic and magnetic devices operating at partial loads, control of DC bus voltage level has been a known technique for decades. With soft magnetic materials (e.g., machines or filter inductors), optimal control of DC voltage is found to reduce losses due to reduction in power converter output current ripple (and consequently reduction in peak flux density) [4]-[6]. Since active control of DC voltage also reduces voltage stress over the power converter itself, further reductions in electric drive losses are achieved, especially when operating at low loads [7]. Recently, with increased research activity on hybrid power systems for electric vehicles, the active control of DC voltage has regained high attention due to impacts on reducing total system losses [8]-[11].

The method used in [8]-[11] controls the DC link voltage as a function of the propulsion drive operating point. Such approach is not feasible in marine applications due to the higher hotel and auxiliary loads that require constant voltage and frequency. Therefore, the DC voltage cannot be varied without significantly impacting the sizing of the converters. To that end, a novel approach to DC voltage control method to minimize drivetrain losses in hybrid FC and battery marine systems was proposed in [12]. Comparing the fuel cell terminal voltage to the DC link, the power system operating modes may be categorized into three; Buck, Freewheel, and Boost modes. In marine power system applications, it is expected that a significant portion of the time, the power system will operate in Freewheel mode and the losses can be reduced by up to 28% compared to operation with a conventional fixed DC bus voltage, as shown in [12].

This work continues the research started in [12] in the following three aspects. First, a new voltage control method based on nonlinear FC voltage model to improve the robustness and reliability of FC current control in the Freewheel mode is set forth. Second, this paper further elaborates the reason Variable DC approach enables significant reductions in power system losses and presents results on typical losses reduction that can be expected. Lastly, this paper presents results demonstrating the additional reduction on FC current ripple due to the use of Variable DC approach which is known to cause extra heat losses in the FC and have negative impacts on the FC durability [13], [14].

The new technical contributions in the presented paper are as follows. First, the paper proposes operation of FC converters in Freewheel mode to eliminate switching losses in the converters, which improves the total drivetrain efficiency, and directly results in reduced fuel consumption. In the Freewheel mode, the control of FC power is managed via external control of DC bus voltage. As the second technical contribution, this paper proposes a new model-based voltage control method for optimal control of DC bus voltage. For a case study presented in this work, the fuel savings achieved with the proposed method are up to 1.87 %-p compared to traditional operation with fixed DC bus voltage.

This paper is organized as follows. Section II presents a short introduction into a typical marine power system and its components. The proposed DC bus voltage control method is set forth in Section III. The test setup used for validation of the Variable DC approach is described in Section IV. The results of the proposed approach are presented in Section V. The paper concludes with discussion and recommendations of future research in Section VI.

II. Description of The Marine Power System

The Variable DC approach is developed for various small to mid-size passenger ships utilizing FCs and batteries as primary power sources and low voltage DC for onboard power distribution. In particular, the approach is suitable for inland waterway vessels where the load power conditions vary significantly during a trip and operation at low speeds/powers is typical [15]. For example, a representative operation profile for a bulk carrier operating for 73 hours in the Rhône river is presented in Fig. 1. The total propulsion power of the vessel is 650 kW and the average speed is 5.19 knots. The maximum hotel power consumption is ~60 kW.

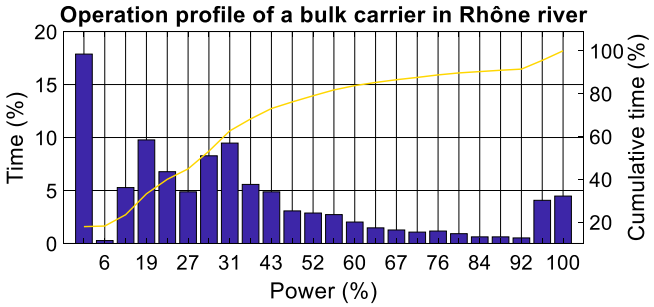

Fig. 1. Operational profile of a bulk carrier in Rhône river [15]. The bars show load power distribution in a single trip. The curve shows cumulative load distribution.

While most of the inland waterway vessels are still typically diesel mechanical shaft-line propulsion vessels, the first step towards decarbonization would be to convert into full electric propulsion systems powered by green power sources using hydrogen FCs and batteries. For example, a generic hybrid FC and battery marine power system suitable for these vessel types is illustrated in Fig. 2. The system is divided into two identical sections for redundancy which is typically required by the authorized classification societies. With identical power sections the total power production requirement per section is 355 kW (total propulsion and hotel load).

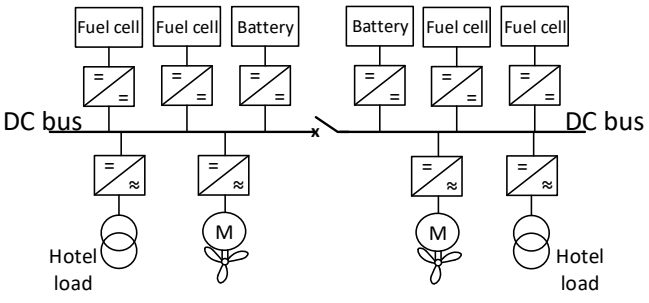

Fig. 2. An FC powered marine vessel system with DC distribution. Apart from propulsion, all other load (e.g., lighting and air conditioning) is considered hotel load.

The propulsion motors are three-phase induction machines with 330 kW and 500V as nominal power and voltage, respectively. The machines are supplied by VSIs. The VSIs are connected to a common DC bus with 720V as nominal DC voltage. The characteristics (i.e., voltage, power and torque) of the propulsion drive as a function of speed are illustrated in Fig. 3. The propulsion load is modeled by means of widely used Wageningen B series of propellers. Large amount of data on these propellers is available in [16], [17].

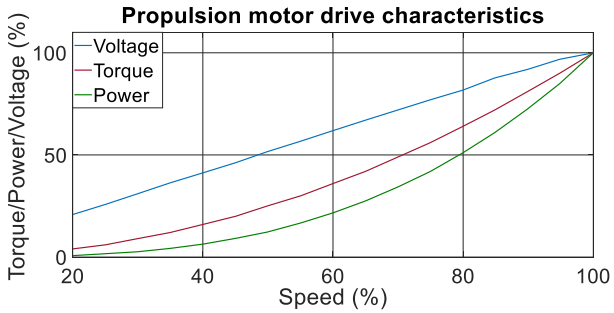

Fig. 3. Characteristics of a propulsion motor drive. Nominal torque and speed of the motor are 2040 Nm and 1480 rpm, respectively.

In the system from Fig. 2, the FCs are operated as main power sources and the batteries are used to provide enhanced dynamic support during fast load transients for the FCs. For increased power redundancy, two smaller FCs are used per section, instead of one larger unit. In inland waterways where shipping lanes are narrow, the risk of losing significant power capacity due to a single failure should be minimized. In applications where the redundancy requirements are not as stringent, one FC per section would suffice. However, another advantage of using more than one FC per section is it enables better optimization of system efficiency by starting and stopping FC units according to the power consumption.

In this work, each FC unit is rated at 185 kW. The voltage characteristics of the FC are illustrated in Fig. 4. Therein, it can be seen the significant FC terminal voltage variation as a function of current. In this system, the voltage of the FC is intentionally dimensioned such that open circuit (i.e., zero current) voltage is above nominal DC voltage and full load voltage is below the nominal DC voltage. The reasons will be further explained in Section III. A buck-boost type DC/DC converter is used to regulate the DC voltage between the FC and the DC bus. The detail of the buck-boost converter operation is available in [12].

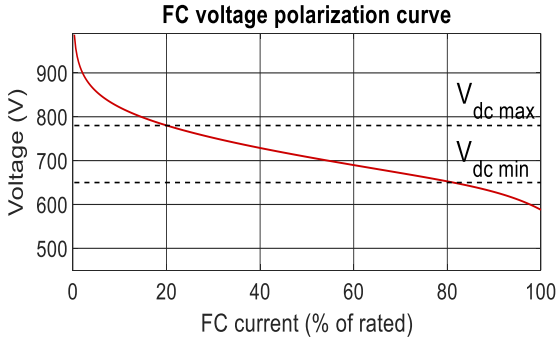

Fig. 4. An FC polarization curve, where V_{dc_min} and V_{dc_max} are minimum and maximum DC bus operation voltages, respectively.

Compared to FCs, batteries have typically much faster dynamic characteristics. They can be used to supply quick load power transients which may not be possible with FCs due to the slowness in their fuel supply systems. If sudden load changes with short time constants are applied on FCs, they may experience fuel starvation, which is known to decrease the FC performance and life time, and may potentially lead to a system blackout [18], which is not acceptable in marine applications. In a marine power system, the worst-case power transient typically occurs if a fully loaded power source fails. In this scenario, the load is instantly transferred from the faulty power source to the healthy ones. Since FCs should be protected from large power transients, the batteries are designed to absorb the full load of a faulty FC.

In this work, the power producing capacities of the batteries are dimensioned such that at 4C discharge rate, the two batteries can together supply full load power of a single FC. The 4C rate is used as a maximum current rate because it is found to not significantly compromise the battery lifetime if the current rate is used rarely and only for short periods [19]. Therefore, the batteries are rated at ~25kWh (46 Ah). Their voltage characteristics as function of current and SOC are illustrated in Fig. 5.

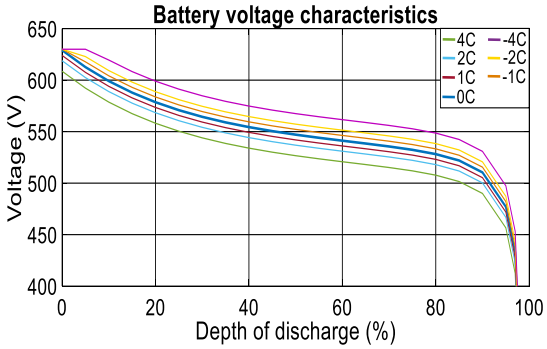

Fig. 5. Battery voltage characteristics as function of SOC and current.

III. The Variable DC Approach

A. General philosophy

In electric land-going vehicles, it is common to actively control the DC supply voltage of a motor inverter for improved efficiency. As shown in Fig. 3, the motor input voltage is proportional to the motor speed. When the motor voltage is lower than the nominal voltage, less supply voltage is needed. The reduction in DC voltage has a positive impact in efficiencies of both the inverter and the motor [20], especially more significant when operating at low speeds. However, as mentioned previously, such an approach is unfeasible in marine applications due to the use of centralized DC distribution systems (i.e., several different loads are connected to the same DC bus). Even if propulsion motors are at standstill, the hotel loads are typically still running and require full DC supply voltage. Therefore, such control strategies are rarely considered in marine vessels.

In [12], a novel Variable DC approach was proposed and targeted specifically towards marine applications. Like the approaches for vehicle applications, this approach too aims of improving total drivetrain efficiency through active control of the DC bus voltage. However, the method is completely different. In this approach, the DC bus voltage is controlled proportionally to the FC voltage as opposed to the propulsion motor voltage, resulting in only slightly varied DC link voltage (± 5-10% around the nominal DC bus voltage) without compromising the power supply to the hotel loads. Similarly, instead of targeting reductions in motor drive losses by varying the DC bus voltage, this method primarily targets reductions in FC converter losses through the voltage variation.

In the proposed approach, FCs are dimensioned such that their open circuit voltages are above nominal DC bus voltage and their full load voltages are below nominal DC bus voltage (see Fig. 4). For the DC bus voltage, minimum (V_{dc_min}) and maximum (V_{dc_max}) values are selected as voltage variation limits. Whenever the FC voltage is within the DC bus voltage operation range, the FC DC/DC converters are controlled into static state (switches closed), which allows free current flow from FC towards the DC bus. With the FC DC/DC converters being static, the FC power is controlled through control of DC bus voltage. Increases in DC voltage lead to decreasing FC power while decreases in DC voltage lead to increasing FC power. In this work, when FC power is controlled by varying the DC bus voltage, the FC unit is said to be in Freewheel mode. Since FC DC/DC converter is kept static, its switching losses are eliminated. However, when the FC voltage is outside the DC bus variation range, DC/DC conversion is required.

In the Variable DC approach, control is divided into three different operating modes: Buck, Freewheel and Boost (naming of the modes is based on the operating principle of FC converter). Buck mode is used whenever FC voltage exceeds V_{dc_max}. Similarly, Boost mode is used whenever fuel cell voltage is below V_{dc_min}. However, when FC voltage is inside DC bus voltage variation range, the FC DC/DC converter is operated in Freewheel mode. In Freewheel mode, the DC bus voltage can be described by [12, eq. (1)]

B. Proposed voltage control method for Freewheel mode

In this work, a new voltage control method is proposed for the Freewheel mode. The method is based on a non-linerar FC voltage model and real-time estimation of FC current. Compared to the PI-controller in [12], the new method provides more accurate FC current control as will be shown in the results section. With the improved control, reduced charging or discharging is required from batteries following a power transient. This reduces battery and battery converter losses, which has an improving impact in drivetrain efficiency. For Buck and Boost modes, the original controllers illustrated in Fig. 6 are retained. Finally, integration of a battery SOC controller to the proposed control method is shown. The SOC controller is important in battery systems for avoiding overly charging or discharging the batteries.

Various models have been proposed for FC voltage control. However, in this work, the empirical voltage model described in [21] and [22] is used to control the DC bus voltage:

$$V_{fc} = N\left(E_{rv} - R_r i_{fc} - A_t \, ln\left(\frac{i_{fc}}{i_0}\right) - m_c e^{n_c i_{fc}}\right). \quad (1)$$

In (1), N represents the number of cells connected in series, E_{rv} is thermodynamically predicted reversible open circuit voltage of the FC and i_{fc} denotes FC current. The second term on the

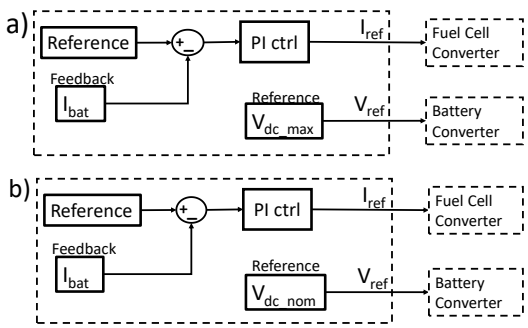

Fig. 6. Control of FC current in a) Buck mode and b) Boost mode. Battery voltage reference is fixed at maximum value and nominal value in Buck and Boost modes, respectively. [12]

right side ($R_r i_{fc}$) models resistive losses due to electron and ion transport in the FC. The third term $\left(A_t\, ln\left(\frac{i_{fc}}{i_0}\right)\right)$ models the activation losses due to reaction kinetics. Finally, the fourth term on the right $\left(m_c e^{n_c i_{fc}}\right)$ models the concentration losses due to mass transport. Usually, mass transport losses have a significant impact on the FC voltage only at high loads (above the nominal power of an FC). Therefore, for operation in the Freewheel mode, mass transport losses can be ignored, thus simplifying the voltage equation to

$$V_{fc} = N\left(E_{rv} - R_r i_{fc} - A_t\, ln\left(\frac{i_{fc}}{i_0}\right)\right). \quad (2)$$

All constants in (2) can be empirically obtained by fitting the equation to a voltage polarization curve data usually found in datasheets from FC manufacturers.

For controlling the power sources, the proposed DC voltage controller uses FCs in order to supply the base power to the system and batteries to compensate for quick load power variations. This can be achieved by adjusting the DC voltage reference V_{ref} of the battery converter to a value, thereby returning the battery to a no-load condition or more specifically, returning the battery converter output current i_{bc} to zero.

Since, at all times, the DC bus voltage equals FC voltage (i.e., $V_{dc} = V_{fc}$), (2) can also be used to describe the instantaneous DC bus voltage as a function of FC current:

$$V_{dc} = N\left(E_{rv} - R_r i_{fc} - A_t\, ln\left(\frac{i_{fc}}{i_0}\right)\right). \quad (3)$$

Whenever (e.g., following a load transient) $i_{bc} \neq 0$, the DC bus voltage must be adjusted to a value which returns the i_{bc} to zero. The new DC bus voltage value (i.e., the reference) can be selected by adding a difference term, ΔV, to the V_{dc} as follows:

$$V_{ref} = V_{dc} + \Delta V. \quad (4)$$

Controlling the DC bus voltage to V_{ref} results in the FC current also changing to a new value, i_{fc2}, which is the sum of the instantaneous battery current and the actual FC current (i.e., $i_{fc2} = i_{bc} + i_{fc}$). Therefore, if V_{dc} and i_{fc} in (3) are substituted by V_{ref} and i_{fc2}, respectively, V_{ref} can also be described by the following FC voltage model:

$$V_{ref} = N\left(E_{rv} - R_r i_{fc2} - A_t\, ln\left(\frac{i_{fc2}}{i_0}\right)\right). \quad (5)$$

Inserting (3) and (5) into (4) and solving ΔV yields

$$\Delta V = N\left(-R_r(i_{fc2} - i_{fc}) - A_t(\ln\left(\frac{i_{fc2}}{i_0}\right) - \ln\left(\frac{i_{fc}}{i_0}\right)\right), \quad (6)$$

which further simplifies to

$$\Delta V = N\left(-R_r i_{bc} - A_t \ln\left(\frac{i_{bc}}{i_{fc}} + 1\right)\right). \quad (7)$$

The final voltage reference equation can be obtained by inserting (7) into (4) as follows:

$$V_{ref} = V_{dc} - N\left(R_r i_{bc} + A_t \ln\left(\frac{i_{bc}}{i_{fc}} + 1\right)\right). \quad (8)$$

The V_{dc} is obtained as a feedback signal from the battery converter. Therefore, as long as the instantaneous FC current (i_{fc}) is known, the required voltage reference for returning i_{bc} to zero can be obtained using (8). One way to obtain i_{fc} is by using measurement feedback (e.g., from the FC converter). However, this requires communication between the voltage controller and each FC converter unit connected to the DC bus. Due the requirement for multiple communication links, the controller can thus become vulnerable to communication failures.

An alternative is to numerically estimate the current from (3). In this work, the Newton-Rhapson method [23] is applied to (3) for numerically estimating the FC current as follows:

$$\hat{\imath}_{fc} = \hat{\imath}_{fc\_prev} - \frac{N\left(E_o - R_r i_{fc\_prev} - A_t\, ln\left(\frac{i_{fc\_prev}}{i_0}\right)\right) - V_{dc}}{N\left(-R_r - \frac{A_t}{i_{fc\_prev}}\right)}. \quad (9)$$

Using (9), the FC current is estimated by the voltage controller during each controller cycle, where $\hat{\imath}_{fc\_prev}$ is the FC current estimated during each previous cycle. The notation ^ is used to indicate that the value is an estimation, instead of a measurement. By replacing i_{fc} in (8) by $\hat{\imath}_{fc}$, it is possible to calculate the DC bus voltage reference as a function of battery converter output current.

In order to meet the requirements for current control (i.e., constant regulated current ramp rate) specific to FCs [24], possibility to easily and reliably control the FC current ramp rate is usually reqired. From (8), it can be noticed that the voltage control method is additive in nature (i.e., a voltage correction term proportional to i_{bc} is constantly added to the DC bus voltage). In this work, since the voltage control is implemented in a digital controller, the correction term is added to the DC bus voltage during each controller cycle. Therefore, the following equation can be written for the FC current ramp rate (A/s):

$$r_i = f_{ctrl} * i_{bc}, \quad (10)$$

where f_{ctrl} expresses the control cycle frequency. If the FC current ramp rate is wanted to be limited to a certain value r_i, before inserting the i_{bc} into (8), it must be limited as follows:

$$i_{bc} = MAX\left(\frac{r_i}{f_{ctrl}}, i_{bat}\right), \quad (11)$$

where i_{bat} is the actual battery current. Since in (8) the correction term added to the DC bus voltage is proportional to i_{bc}, limiting i_{bc} to a value (dependent on the ramp rate and controller sample frequency) obtained in (11) enables FC current to be robustly controlled by a selected ramp rate.

Finally, with the FC current control design ready, a battery SOC controller is needed. A simple way to achieve SOC control is to add another controller (e.g., a PI type) which outputs a battery current reference based on the difference between SOC reference and actual SOC. The output reference is subtracted from i_{bat}, and the result is inserted into the Eq. (11). That way, instead of controlling the i_{bat} to zero, it is controlled to a value requested by the SOC controller. If SOC control is not needed and its output is zero, the i_{bat} gets controlled to zero. SOC control can also be performed in Buck and Boost modes using similar control scheme. In the two modes, the output of the SOC controller is given as a current reference to the PI controllers of the FC current (see. Fig. 6). However, since this work focuses on describing and validating the Variable DC Approach method, SOC control will not be discussed further.

A high-level diagram of the battery converter and FC converter in Freewheel mode is illustrated in Fig. 7. The FC voltage model, the FC current estimator and the current limit are implemented using Eqs. (8), (9) and (11), respectively. The SOC controller can be a PI controller (as discussed above) or any other functional SOC controller which proides a proper battery current reference for the SOC control. The FC converter allows free flow of current from the FC towards the DC bus.

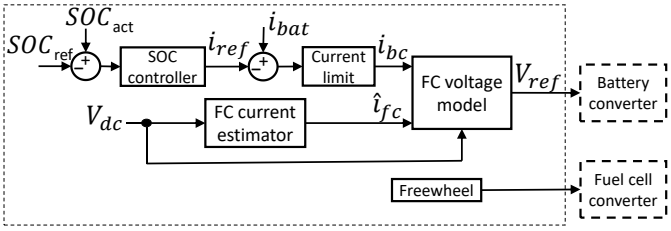

Fig. 7. A high-level diagram of the proposed voltage controller in Freewheel mode.

IV. Hybrid Power System Setup For HIL Testing

In order to validate the functionality of the Variable DC approach, a real-time hardware-in-loop (HIL) test setup was built as illustrated in Fig. 8. In the setup, two FCs, a battery, a propulsion motor and power stages of four power converters (three DC/DC and one DC/AC) are virtually modeled. Two HES880 [25] control units are connected to the HIL simulator through hardwired inputs and outputs (IOs). The IOs are connected between the IGBT gate control interfaces of the HES units and the highspeed control IO of the HIL simulator. Through the IOs, the HES880 units control the virtual power stages of battery converter and VSI. The power stages of FC converters are controlled by virtual controllers using control methods described in Section III. The simulation sample times used for the power stage simulation and the FC converter control are $1\mu s$ and $50\mu s$, respectively. In the following section, the models used in this work are described. Additional details on the functional principle of HIL testing is available in [26].

A. Power sources

The power sources used in this work are proton exchange membrane (PEM) FCs and lithium ion (Li-ion) batteries. PEM FCs are low temperature FCs often used in transport applications (i.e. electric cars, trains, busses, etc.). For dynamic

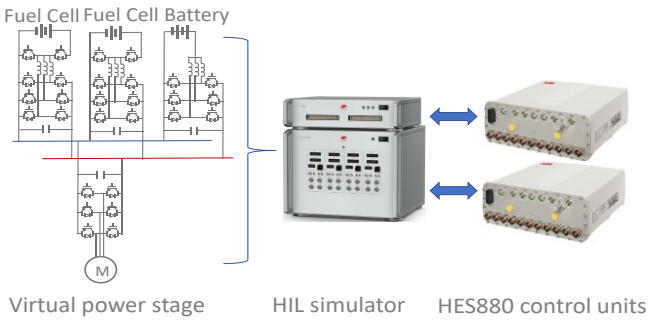

Fig. 8. A HIL test setup consisting of two FC units, a battery unit and a propulsion motor unit.

and steady state modelling of a PEM FC, this work will use an equivalent circuit model presented and validated in [27]. All parameters required by the dynamic PEM fuel cell model are presented in [12, Tab. 1]. The voltage characteristics of the FC were previously presented in Fig. 4.

Lithium ion (Li-ion) batteries are common battery types used in transportation applications due to their high energy and power density. The dynamic model used in the HIL tests is a Li-ion battery model from the Typhoon HIL library [26]. The voltage characteristics of the battery were previously presented in Fig. 5.

Both the battery and the FCs are connected to the common DC bus through DC/DC converters. The battery converter is an interleaved three-phase bidirectional DC/DC converter. It is controlled by a real HES880 control unit with a DC/DC conversion control software. The switching frequency of the HES880 DC/DC converter is 5 kHz. It is a default value optimized for the product and therefore, not changed in this work. The FC DC/DC converter is a unidirectional buck-boost converter illustrated in Fig. 9. The switching frequency of the FC DC/DC converter is the same as that of the battery converter. Details of the used passive components and converter switches have been presented in [12].

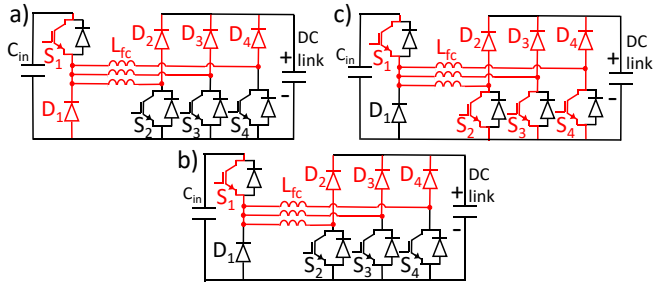

Fig. 9. FC converter diagram and its operation modes: a) Buck mode (S_1 in PWM, S_2-S_4 off), b) Freewheeling mode (S_1 constantly on, S_2-S_4 off) and c) Boost mode (S_1 constantly on, S_2-S_4 in PWM). [12]

B. Propulsion motor drive

The propulsion motor type used in this work is a three-phase induction motor. Both the motor and the power stage of the VSI are HIL models from the Typhoon HIL library [26]. The inverter is controlled by a HES880 control unit with primary control software. The switching frequency of the HES880 for motor inverter is 3 kHz. It also is a default value optimized for the product and not changed for this work. The motor parameters used in this work are presented in Table 1.

Typically, motor losses contribute to a significant portion of total drivetrain losses in propulsion applications. In different variable DC control methods proposed for land going vehicles, reduction in motor iron losses is used as a major argument for the DC voltage control. However, the efficiency improvements are mainly significant when operating at lower motor speeds [20]. The reason is that at lower speeds, the required motor input voltage is also low (see. Fig. 3), and thus allowing significant reduction in DC bus voltage. However, at higher speeds where DC bus voltage can be reduced only slightly, the impact in losses is less significant. Experimental validation of this phenomena is found in [28] and [29]. For example, from [29, Fig. 10], any meaningful difference in motor losses between variable DC operation and fixed DC operation occur only when voltage is decreased more than 15% from the nominal voltage.

In the proposed Variable DC approach for marine vessels, the DC bus voltage is varied only ±10% around the nominal voltage. Therefore, the difference in motor losses between the proposed approach and a conventional fixed DC voltage approach is considered insignificant, and thus ignored in the analysis of this work. However, motor inverter losses are included in the analysis.

Table 1: Induction motor parameters used in the HIL tests

Parameter	Symbol	Value
Stator winding resistance	R_{ms}	7.94 $m\Omega$
Stator leakage inductance	L_{mls}	0.12 mH
Rotor winding resistance	R_{mr}	8.23 $m\Omega$
Rotor leakage inductance	L_{mlr}	0.11 mH
Magnetizing inductance	L_{mm}	6.81 mH
Moment of inertia	J_m	2.38 kgm^2

C. Loss models for energy efficiency calculations

Since the Variable DC approach was designed for improved drivetrain efficiency, proper converter and passive component loss models are needed to evaluate the drivetrain efficiency against conventional fixed DC bus systems. The models are pre-validated that utilize energy loss data, typically found in component manufacturer datasheets and summarized in [12]. Experimental validation of the converter loss models has previously been presented in [30]. The converter and battery loss models used in this work are presented in the following.

The IGBT and diode losses are typically divided into switching and conduction losses. The switching losses are calculated as follows:

$$P_{sw}(t) = \frac{u_{dc}(t) i_L(t)}{U_r I_r} f_{sw}(t)(E_{sw}), \tag{12}$$

where u_{dc} is DC bus voltage, i_L is converter phase current and E_{sw} is the sum of IGBT and diode switching losses per switching period at DC voltage U_r and current I_r. For the IGBT type used in this work, the E_{sw} is given for $U_r = 600V$ and $I_r = 600A$ [31]. However, since the DC voltage and converter current vary at different operating points, the energy losses must be properly scaled according to actual DC voltage and current. Hence, in (12) the switching losses are divided by $U_r I_r$ and multiplied by the actual DC voltage u_{dc} and current i_L, so as to obtain the switching losses of IGBTs and diodes at variable DC voltages. The conduction losses are calculated as follows:

$$P_{IGBT\_con}(t) = U_{ce0} i_L(t) + R_{ce0} i_L(t)^2, \tag{13}$$

$$P_{diode\_con}(t) = U_{fw0} i_F(t) + R_{fw0} i_F(t)^2, \tag{14}$$

where i_F is diode forward current, u_{ce0} and u_{fw0} are IGBT and diode threshold voltages, respectively, and R_{ce0} and R_{fw0} are IGBT and diode on-state resistances, respectively.

Inductor winding losses and capacitor losses are calculated using their equivalent series resistances (ESRs) as follows:

$$P_{L\_win}(t) = i_L(t)^2 ESR_L, \tag{15}$$

$$P_C(t) = i_C(t)^2 ESR_C, \tag{16}$$

where i_C is capacitor current. Inductor core losses are calculated using the well-established Steinmetz equation which gives core losses per unit volume as follows:

$$P_{core/V_c} = k {f_{sw}}^a B_m^b, \tag{17}$$

where B_m is peak flux density, V_c is the core volume and constants a, b and k are Steinmetz coefficients. Peak flux density is obtained from the following equation:

$$B_m = \frac{L_{fc} i_p}{N_L A_c}, \tag{18}$$

where i_p is peak inductor current, L_{fc} is inductor inductance, N_L is number of turns and A_c is cross sectional area of the core. All the above-mentioned parameters that will be used in the following HIL tests are available in [12].

The internal battery losses are modeled as resistive losses using the average internal resistance of the battery. The battery losses are obtained as follows:

$$P_{bat\_L} = R_b * i_{bat}^2, \tag{19}$$

where R_b is the average internal resistance of the battery and i_{bat} is the battery current. In marine applications, the efficiency, η, of lithium ion batteries is typically ~99% at nominal current [32]. The battery efficiency at nominal current is described as follows [33]:

$$\eta = 1 - \frac{R_b * I_{bnom}^2}{I_{bnom} E_{bnom}}, \tag{20}$$

where I_{bnom} is nominal current and E_{bnom} is nominal voltage. Hence, for mentioned efficiency, the internal resistance of the battery can be solved from (20). The battery parameters used in the following HIL tests are presented in Table 2.

Table 2: Battery parameters used in the HIL tests

Parameter	Symbol	Value
Nominal DC voltage	E_{bnom}	510 V
Nominal current	I_{bnom}	46 A
Battery capacity	Q_b	46 Ah
Full charge open circuit voltage	$E_{bocv\_100\%}$	617 V
Internal resistance	R_b	0.111 Ω

V. HIL Results And Discussion

A. Fuel cell current control in Freewheel mode

The proposed voltage controller was designed specifically for robust and reliable FC current control in the Freewheel mode. To evaluate the robustness of the controller, its performance is tested against that of the PI controller from [12]. Next, the reliability of the control method in case of a power

source failure is also tested. Finally, the performance of the control method against two differently rated FCs parallel connected in the system is analyzed.

The comparison between the proposed control and PI control is performed via a power cycling test. The test is performed as follows. First, the propulsion power is increased from 30% (of nominal FC power) to 80%. Once the FC has reached the 80% loading, the motor power is returned to 30%. The time for the FC to ramp its power up to 80% and back to 30% was measured. The test is performed with both the proposed control method and the PI-based control method. Both controllers are tuned to achieve 20A/s increasing and 40A/s decreasing FC current ramp rates.

The results of the cycling test are illustrated in Fig. 10. The proposed control method finishes the power cycle in 14.65s while the PI-based method achieves the same in 16.57s (13.1% longer than the proposed method). Because of the improved cycle time, less energy is cycled in and out of the battery, as shown in lower graph of Fig. 10. In this test, the proposed control method resulted in about 23.7% less energy being cycled in and out of the battery compared to the PI controller. The energy difference was calculated by integrating the battery powers over time and subtracting them from each other. For vessels where frequent transients are expected, the improved cycle time can turn into meaningful energy savings.

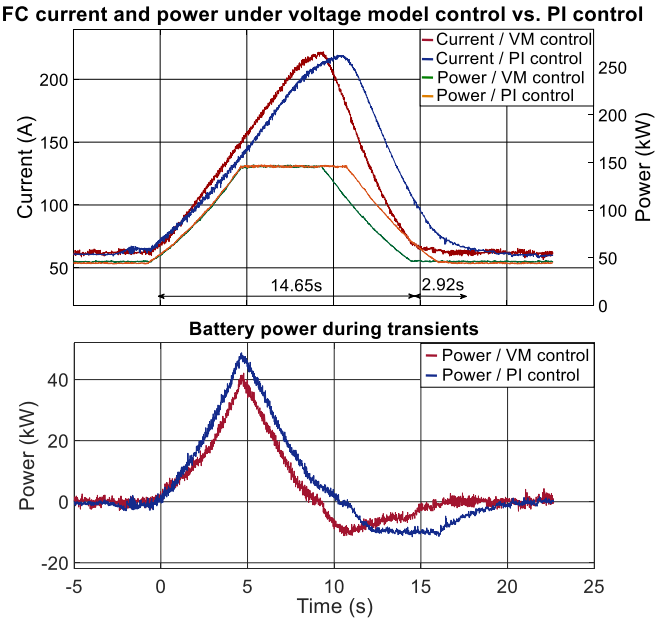

Fig. 10. Power cycling test between the proposed voltage model (VM) controller and the PI controller from [12].

The reliability of the proposed control method is evaluated via a power source failure test. The test scenario is as follows. First, the propulsion power is increased from 30 % (of nominal motor power) to 50%. Once the sum power of FCs equals the motor power, the motor power is returned to 30 %. During this power cycle, only the load sharing between the two FCs is observed. About six seconds after the motor power has returned to 30% it is again increased to 50%. However, this time, during the ramp up of FC power, one of the FCs is intentionally tripped. The reaction of the healthy FC is observed. The results of the test are presented in Fig. 11.

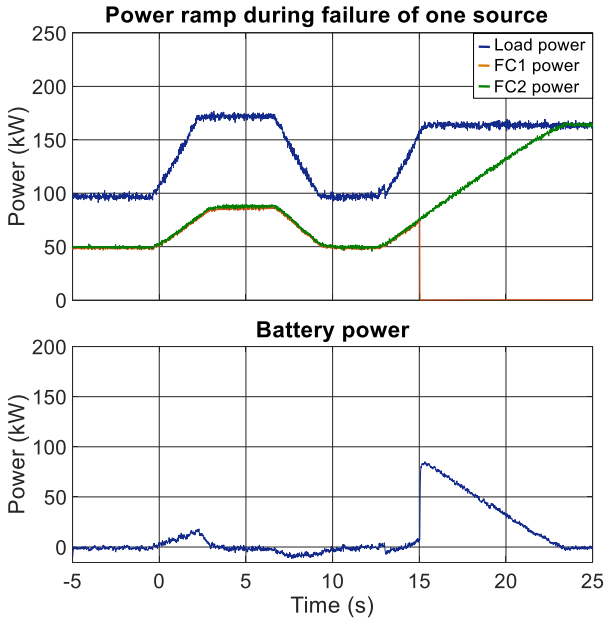

Fig. 11. A power failure test using two FCs. At 15s, FC1 is tripped but operation of the rest of the system is continued.

The results show that load sharing between the two parallel operated FCs works seamlessly and that even during failure of one FC, the healthy FC does not experience any harmful power transients. The results are important because they demonstrate that even though in Freewheel mode the currents of parallel operating FCs are not controlled directly by dedicated converters, the control during both normal and fault conditions is robust and does not expose the FCs to harmful overloading.

Finally, in the last test, the proposed voltage controller is tested with two differently rated FCs in Freewheel mode. This test is important to understand the system performance as the FC ages and its voltage characteristics tend to degrade. Due to the degradation, the electrode activity and membrane condition tend to decrease, which both lead to higher internal FC losses. Consequently, the FC voltage drops. Robust control must be achieved through the whole operating lifetime of the FCs.

For this test, the voltage characteristics of FC1 was reduced by ~5% to mimic a degree of degradation. The voltage controller parameters are maintained to the same value as tuned for the healthier FC. The two FCs are operated in Freewheel mode and dynamic transients are applied to the system. The results of this test are illustrated in Fig. 12. In the first eight seconds of the test, FCs are both in Freewheel mode. As can be expected, the load is unequally shared between the two FCs. Since FC2 is healthier than FC1, it takes more load compared to FC1. However, at about 8s, FC1 is commanded to Boost mode and the actual power of FC2 is given as a reference to the FC1 converter controller. Thus, equal power sharing is achieved. Slightly after 23s, the FC1 is commanded back to Freewheel mode and the load is shared unequally again.

From the three tests performed, the following observations can be made. First, the proposed controller provides improved FC current control accuracy which results into lower power transients for the battery. Although, it should be noted that the control robustness of the PI controller could be improved by modifications (e.g., gain scheduling, linearization or using non-

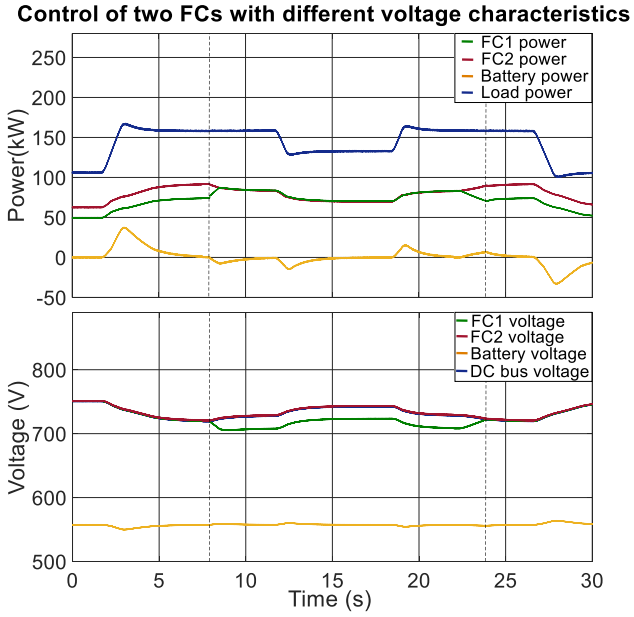

Fig. 12. Control of two differently rated fuel cells in Freewheel mode. Between the dashed vertical lines, the more degraded FC is set to Boost mode to force equal load sharing.

linear PI control) suitable for non-linear control. However, the proposed method offers an advantage. It is straightforward to parametrize by curve-fitting the used voltage model to an FC voltage polarization curve usually found in manufacturer datasheet. Second, since batteries constantly control the DC bus voltage, even in case of an FC failure, the remaining FCs continue operation unharmed. Third, the voltage controller stays robust even if the FC parameters are slightly erroneous, as can be seen from the applied transients. Finally, two differently rated FCs can be operated in Freewheel mode, despite the unequal load sharing between FCs. Nevertheless, even if the load sharing is not equal, it is still recommended to operate in Freewheel mode due to the improved drivetrain efficiency, as will be shown next. In the event where equal load sharing is required, one of the FCs can be set to either Buck or Boost mode to force equal load sharing.

B. Drivetrain efficiency in Variable DC approach

In this section, the drivetrain losses are compared between the proposed Variable DC approach and conventional fixed DC controlled systems. First, the losses in the steady-state conditions at different operating points are analyzed and then followed by assessments of losses during transients using time-domain HIL simulations.

In order to obtain the steady state drivetrain losses, the system is simulated at different power levels and DC voltages. The results of the simulation are shown in Fig. 13. Therein, dark blue color indicates possible operating points with the smallest drivetrain losses. The white area in bottom right corner indicates that DC bus voltage is not enough to produce the motor voltage for the required power. Thus, operation in that area is forbidden. The operating points during Freewheeling mode in the proposed approach are indicated by the magenta line which are within the regions with the lowest drivetrain losses.

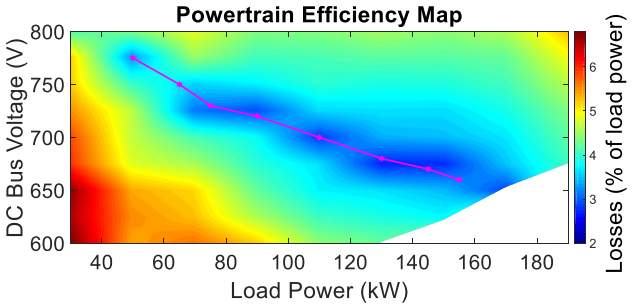

Fig. 13. Total drivetrain efficiency map as function of power and DC bus voltage.

To further evaluate the total drivetrain losses of a system operating with the Variable DC approach, the HIL test setup was operated in Buck, Freewheel and Boost modes. The target was to observe the power levels, the voltage levels and the losses of the drivetrain components in the system. The waveforms of the mentioned quantities are presented in Fig. 14. The powers of FC, battery and propulsion motor (load) are illustrated in Fig. 14a. The vertical gray lines highlight the transitioning between the different operating modes. Similarly, the FC, battery and DC bus voltages are shown in Fig. 14b. Finally, the total drivetrain losses are presented in Fig. 14c. The losses considered are those of FC converter, motor inverter, battery and battery converter. The rapid transients in losses at 13s and 54s are caused by high power charging/discharging of the battery. During steady states (i.e., battery power is about zero), the figure shows that relative losses in Freewheel mode are significantly lower than those in both Buck and Boost modes (modes with fixed DC voltage). The main loss reduction factor in the Freewheel mode is the absence of high frequency switching in the FC converter, which eliminates the switching losses in the FC converter semiconductors and core losses in the passive components of the FC converter.

According to the presented results, the Variable DC approach (more specifically, Freewheel mode) provides a significant efficiency boost to a hybrid power system operating with FCs and batteries. However, to properly evaluate the advantages of the Variable DC approach, the total drivetrain efficiency of a system operating with the Variable DC approach must also be compared to that of the system operating with a fixed DC bus voltage, which is at the moment the state of the art in marine vessel systems. To achieve this, the HIL setup was operated at six different operating points with both the Variable DC approach and the fixed DC approach. In fixed DC approach, the DC bus voltage was kept at nominal voltage (i.e., 720 V). The losses at different operating points are presented in Table 3. The losses in both modes are categorized into FC converter losses and load converter losses to illustrate the components where the major efficiency improvements occur. Since the data provided in Table 3 is obtained from different steady-state simulations, battery power is about zero and no difference can be observed in battery and battery converter losses between the two control methods. Therefore, these losses are excluded from Table 3.

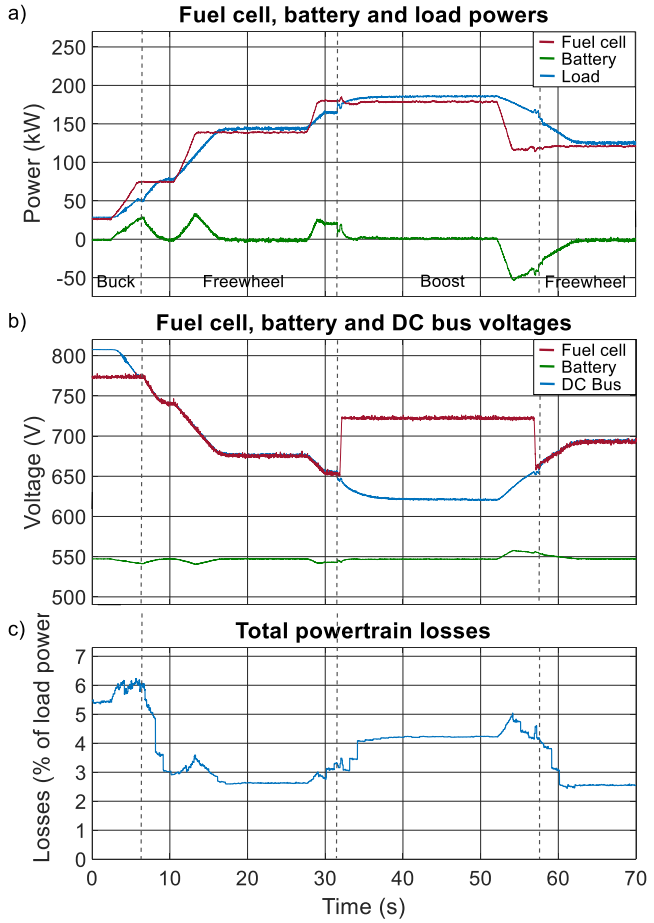

Fig. 14. a) Power, b) voltage and c) losses of drivetrain components during different operating modes when operated with variable DC Approach. Optimal efficiency is achieved in Freewheel mode.

Table 3: Comparison of steady-state drivetrain losses between Variable DC Approach and conventional fixed DC approach.

	Losses with fixed DC approach			Losses with Variable DC approach			
FC Power (kW)	FC conv. (kW)	Load Conv. (kW)	Operation mode	FC conv. (kW)	Load Conv. (kW)	Operation mode	Diff. (%)
25	0.87	1.05	Buck	0.40	1.15	Buck	-19
55	0.97	1.55	Buck	0.20	1.61	Freewheel	-28
102	1.46	2.39	Boost	0.46	2.39	Freewheel	-26
133	1.66	2.71	Boost	0.70	2.68	Freewheel	-23
161	2.63	3.42	Boost	1.00	3.33	Freewheel	-28
188	4.05	3.90	Boost	4.05	3.90	Boost	0

According to the values presented in Table 3, the Variable DC approach offers improved efficiency over a system utilizing fixed DC voltage control. In particular, the Freewheel mode reduces total drivetrain losses by up to 28 %. The improvements in efficiency are consistent across the complete operating range of the Freewheel mode. Most of the efficiency increase occurs in the FC converter, while the battery and load converter losses are only marginally impacted by the variation in the DC bus voltage. The reason for small impact on the load converter losses is the relatively small variation of the DC bus voltage, which is only ± 10% from nominal. Nevertheless, for the FC converter, the aforementioned voltage variation is significant because it allows bypass of the power conversion between the FC and the DC bus, and thus significantly reducing the total system losses.

Recall that the main motivation of the work is to improve hydrogen fuel consumption in order to facilitate wider adoption of such technology in the marine market. The efficiency improvement results presented in this work are highly correlated to the hydrogen fuel savings. For example, a river-going vessel with an operation profile shown in Fig. 1 has a total energy requirement of about 18.4 MWh per round trip. With a conventional fixed DC approach, the total drivetrain losses are about 760 kWh, while with the proposed Variable DC approach, only about 605 kWh. Therefore, about 155 kWh (or 0.84% of the total load consumption) is saved by adopting the proposed approach. Considering that the efficiencies of commercial FCs normally range between 0.45 and 0.55, the total impact in hydrogen fuel consumption would be between 1.53 %-p and 1.87 %-p for the aforementioned operation profile. In terms of kilograms, the hydrogen fuel savings would be approximately 8.5 - 10.3 kg per round trip. Assuming 100 round trips per year, the yearly savings corresponds to 850 - 1030 kg. Due to adoption of hydrogen as fuel for marine vessels being still at its infancy, determination of accurate price for hydrogen fuel is difficult. However, as an example, the cost of hydrogen is estimated to be 5.43 – 7.40 $/kg in San Francisco area if produced from non-renewable energy sources [1]. Using the price estimate as reference, yearly fuel savings for the vessel studied in this work would be about $4616 – $7622. Noting that total energy consumption of larger vessels operating in the same area can be up to 15 times higher than that presented in this work, the monetary savings for these vessels are substantial. Thus, the proposed approach enables significant operational cost reductions for a vessel operator.

C. Fuel cell current ripple in Variable DC Approach

Earlier, it was mentioned that FCs are known to be sensitive to current ripples. They cause extra heating in the FC due to increased energy losses and in the long run it may lead to quicker degradation of the FC. Since FC current is not directly controlled by the FC converter in the Freewheel mode, it is important to evaluate the impacts of operating in this mode to the current ripple at the FC terminals. Thus, the HIL setup was used to measure both high-frequency (HF) ripple (> 1 kHz) and low-frequency (LF) ripple (10-100Hz) in the FC current at the different Variable DC approach operating modes.

The HF current ripple at the FC terminals is illustrated in Fig. 15. Compared to Buck and Boost modes (i.e. modes where FC current is controlled directly by the FC converter), the HF current ripple is nonexistent in the Freewheel mode, mainly due to two reasons. First, since FC conversion is bypassed, the ripple that would normally be generated by the switching of the FC converter is not present. Second, the HF ripple generated by other switching components connected to the DC bus (e.g. load or battery converter) is effectively filtered by the combination of DC bus capacitance and FC converter inductor.

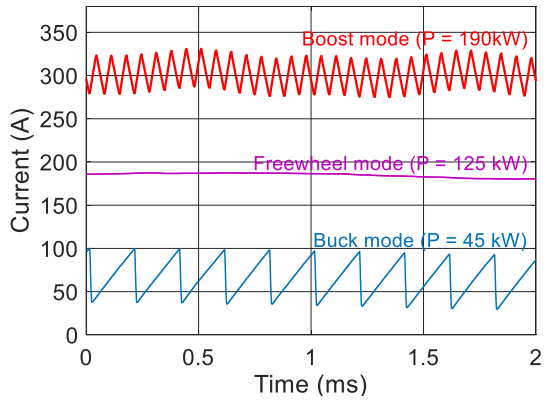

Fig. 15. HF current ripple at the FC output. In Freewheel mode, the HF ripple is filtered by the DC bus capacitors and the inductor of FC converter.

The LF ripple in the FC current is illustrated in Fig. 16. Compared to Buck and Boost modes, the LF current ripple is comparable in the Freewheel mode. The maximum LF peak to peak ripple values are 7.5A, 5.5A and 5.8A in Buck, Freewheel and Boost modes, respectively. In Buck and Boost modes, the amount of LF current ripple applied to the FC depends mainly on the current control robustness of the FC converter. On the other hand, in the Freewheel mode, the amount of current ripple mainly depends the voltage control robustness of battery converters, the amount of capacitance in the DC bus and the type of loads connected to the common DC bus. Due to large size of the DC bus capacitance and high robustness of the battery converter voltage control, the LF current ripple at FC terminals is similar in the Freewheel mode as in Buck and Boost modes. Therefore, it can be concluded that operation in Freewheel mode has no significant impact on LF current ripple at the FC terminals

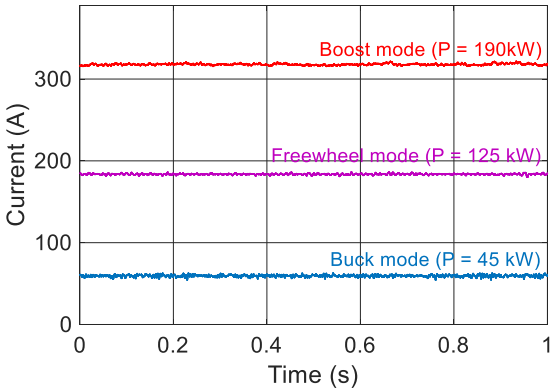

Fig. 16. LF current ripple at the FC output. No significant difference can be noticed in the current ripples between different modes. The maximum LF peak to peak ripple values are ca. 7.5A, 5.5A and 5.8A for Buck, Freewheel and Boost modes respectively.

VI. Conclusions

This work has proposed a novel control method for hybrid FC and battery power systems in marine vessels. The new technical contributions of the paper are operation of FC converters in Freewheel mode and the new model-based control method proposed for variable DC voltage control. The Variable DC approach was shown to significantly reduce losses (up to 28% compared to a system with fixed DC voltage) in electric drivetrain equipment. For the example operational profile, the efficiency improvement directly translates to reduction of hydrogen fuel consumption by up to 1.87%-p, and thus providing significant savings for vessel operators. Additionally, operating in Freewheel mode was shown to eliminate the HF current ripple from the FC output, which can have further positive impacts on the FC losses and durability, which translates to reduction in capital expenditure for the vessel owner.

The concept presented in this paper is being developed for future zero-emission marine vessels that are powered by FCs and batteries. Currently, the presented concept is in the development and feasibility evaluation stage. For future research and further improvement in system level efficiency, a vessel power and energy management system utilizing the Variable DC approach can be further studied. For example, methods (e.g., load forecasting) to track optimal efficiencies during different vessel load profiles will be studied.

References

[1] J. W. Pratt and L. E. Klebanoff, "Feasibility of the SF-BREEZE: a zero-emission, hydrogen fuel cell, high-speed passenger ferry," Sandia National Laboratories, Livermore, California, 2016.

[2] T. I. B∅, A. Swider and E. Pedersen, "Investigation of drivetrain losses of a DP vessel," *2017 IEEE Electric Ship Technologies Symposium (ESTS)*, Arlington, VA, 2017, pp. 508-513.

[3] O. L. Osen, "Optimizing electric energy production on-board offshore vessels: Vessel power consumption profile and production strategies using genetic algorithms," in *OCEANS*, Shanghai, 2016, pp. 1-10.

[4] A. Boglietti, P. Ferraris, M. Lazzari and F. Profumo, "Effects of different modulation index on the iron losses in soft magnetic materials supplied by PWM inverter," in *IEEE Transactions on Magnetics*, vol. 29, no. 6, pp. 3234-3236, Nov. 1993.

[5] A. Krings, J. Soulard and O. Wallmark, "PWM Influence on the Iron Losses and Characteristics of a Slot-less Permanent Magnet Motor with SiFe and NiFe Stator Cores", IEEE Transactions on Industry Applications, Vol. 51, pp. 1475 – 1484, 2014.

[6] A. Boehm and I. Hahn, "Influence of pulse width modulation (PWM) on the iron losses of electrical steel," *International Power Electronics Conference*, Hiroshima, 2014, pp. 283-288.

[7] C. Yu, J. Tamura and R. D. Lorenz, "Optimum DC Bus Voltage Analysis and Calculation Method for Inverters/Motors With Variable DC Bus Voltage," in *IEEE Transactions on Industry Applications*, vol. 49, no. 6, pp. 2619-2627, Nov.-Dec. 2013.

[8] K. K. Prabhakar, M. Ramesh, A. Dalal, C. U. Reddy, A. K. Singh and P. Kumar, "Efficiency investigation for electric vehicle powertrain with variable DC-link bus voltage," *42nd Annual Conference of the IEEE Industrial Electronics Society*, Florence, 2016, pp. 1796-1801.

[9] S. Tenner, S. Gimther and W. Hofmann, "Loss minimization of electric drive systems using a DC/DC converter and an optimized battery voltage in automotive applications," *IEEE Vehicle Power and Propulsion Conference*, Chicago, IL, 2011, pp. 1-7.

[10] T. Schoenen, M. S. Ku nter, M. D. Hennen and R. W. De Doncker, "Advantages of a variable DC-link voltage by using a DC-DC converter in hybrid-electric vehicles," *IEEE Vehicle Power and Propulsion Conference*, Lille, 2010, pp. 1-5.

[11] M. Farasat, A. Arabali and A. M. Trzynadlowski, "Flexible-Voltage DC-Bus Operation for Reduction of Switching Losses in All-Electric Ship Power Systems," in *IEEE Transactions on Power Electronics*, vol. 29, no. 11, pp. 6151-6161, Nov. 2014.

[12] A. Haxhiu, J. Kyyrä, R. Chan and S. Kanerva, "A variable DC approach to minimize drivetrain losses in fuel cell marine power systems," *IEEE Power and Energy Conference at Illinois (PECI)*, Champaign, IL, 2019, pp. 1-6.

[13] B. Wahdame, L. Girardot, D. Hissel, F. Harel, X. François, D. Candusso, M. Pera and L. Dumercy, "Impact of power converter current ripple on

the durability of a fuel cell stack," *IEEE International Symposium on Industrial Electronics*, Cambridge, 2008, pp. 1495-1500.

[14] G. Fontes, C. Turpin, S. Astier and T. A. Meynard, "Interactions Between Fuel Cells and Power Converters: Influence of Current Harmonics on a Fuel Cell Stack," in *IEEE Transactions on Power Electronics*, vol. 22, no. 2, pp. 670-678, March 2007.

[15] B. Kelderman et al., "PROMINENT - D1.1 List of operational profiles and fleet families", European comission, 2016.

[16] M. Bernitsas, D. Ray, P. Kinley, "KT, KQ and Efficiency Curves for the Wageningen B-Series Propellers", University of Michigan, 1981.

[17] G. Kupier, "The Wageningen Propeller Series", MARIN Publ., The Netherlands, 1992.

[18] L. He, Z. Han, Y. Liu, Z. Niu and Z. Liu "Effects of Gas Starvation on Performance of a Single PEMFC", IEEE Transportation Electrification Conference and Expo, Asia-Pacific, 2017, pp. 1-5.

[19] D. Stroe, M. Swierczynski, S. Kær and R. Teodorescu, "Degradation Behavior of Lithium-Ion Batteries During Calendar Ageing—The Case of the Internal Resistance Increase," in IEEE Transactions on Industry Applications, vol. 54, no. 1, pp. 517-525, Jan.-Feb. 2018.

[20] J. Estima and A. Cardoso, "Efficiency Analysis of Drive Train Topologies Applied to Electric/Hybrid Vehicles," in IEEE Transactions on Vehicular Technology, vol. 61, no. 3, pp. 1021-1031, March 2012.

[21] J. Larminie and A. Dicks, Fuel cell systems explained, 2nd ed., Chichester: John Wiley & Sons Ltd., 2003, pp. 45 – 66.

[22] R. O'Hayre, S. Cha, W. Colella and F. Prinz, FC Fundamentals, 1st ed., Hoboken, John Wiley & Sons Inc., 2016.

[23] R. Adams, Calculus: A Complete Course, 6th ed., Toronto, Pearson Addison Wesleay, 2006.

[24] J. Moré, P. Puleston, C. Kunusch and M. Fantova, "Development and Implementation of a Supervisor Strategy and Sliding Mode Control Setup for Fuel-Cell-Based Hybrid Generation Systems," in *IEEE Transactions on Energy Conversion*, vol. 30, no. 1, pp. 218-225, March 2015.

[25] ABB Oy, "HES880 Mobile Drive", 2018. [Online]. Available: https://new.abb.com/drives/low-voltage-ac/industry-specific-drives/hes880. [Accessed: 01- Nov- 2018]

[26] Typhoon HIL, "Typhoon HIL schematic library", 2018. [Online]. Available:https://www.typhoon-hil.com/products/hil-software/schematic-editor. [Accessed: 17- Dec- 2018]

[27] I. San Martin, A. Ursua and P. Sanchis "I. San Martin, A. Ursua and P. Sanchis, "Modelling of PEM fuel cell performance: Steady-state and dynamic experimental validation," Energies, Vol. 7, pp. 670-700, 2014.

[28] A. Boglietti, A. Cavagnino, D. Ionel, M. Popescu, D. Staton and S. Vaschetto, "A General Model to Predict the Iron Losses in PWM Inverter-Fed Induction Motors," in IEEE Transactions on Industry Applications, vol. 46, no. 5, pp. 1882-1890, Sept.-Oct. 2010.

[29] G. Sousa, D. Simonetti and E. Norena, "Efficiency optimization of a solar boat induction motor drive," Conference Record of the 2000 IEEE Industry Applications Conference. Thirty-Fifth IAS Annual Meeting and World Conference on Industrial Applications of Electrical Energy (Cat. No.00CH37129), Rome, Italy, 2000, pp. 1424-1430 vol.3

[30] L. Aarniovuori, L. I. E. Laurila, M. Niemela and J. J. Pyrhonen, "Measurements and Simulations of DTC Voltage Source Converter and Induction Motor Losses," in IEEE Transactions on Industrial Electronics, vol. 59, no. 5, pp. 2277-2287, May 2012.

[31] 'Technical information for IGBT module FF600R12IP4', Infinen 2018. [Online]. Available: https://www.infineon.com/dgdl/Infineon-FF600R12IP4-DS-v02_04-en_de.pdf?fileId=db3a30431f848401011feb94350f3eb9

[32] B. Perry, "High capacity battery packs", ABB Generations, white paper, [Online]. Available: https://library.e.abb.com/public/82b8e284d5fdc935c1257a8a003c26a4/ABB%20Generations_22%20High%20capacity%20battery%20packs.pdf

[33] O. Tremblay, L. Dessaint and A. Dekkiche, "A Generic Battery Model for the Dynamic Simulation of Hybrid Electric Vehicles," IEEE vehicle power and propulsion conference, 2007, pp. 284-289.

Arber Haxhiu (M'2020) received his B.Sc. and M.Sc. degrees from the Aalto University, Helsinki, Finland, in 2015 and 2016, respectively. Currently, he is working towards the D.Sc degree in the field of industrial electronics and electrical drives.

Since 2014, he has held various positions in technology and product development at ABB. Currently, he works as an R&D Senior Engineer in the technology development at ABB Marine & Ports. His research interests include hydrogen fuel cells and their application in marine power systems.

Jorma Kyyrä (M'1994) received the M.Sc., Lic.Sc., and D.Sc. degrees from the Helsinki University of Technology (TKK), which is now Aalto University, Helsinki, Finland, in 1987, 1991, and 1995, respectively.

Since 1985, he has been with the university in various positions. Since 1996, he has been an Associate Professor of power electronics, and since 1998, a Professor of power electronics. From 2008 to 2009, he has been the Dean with the Faculty of Electronics, Communications and Automation, TKK, and from 2009 to 2011, the Vice President of Aalto University, Espoo, Finland. He is currently the Head of the Department of Electrical Engineering and Automation with Aalto University. His research interest is power electronics at large. The power electronics group at Aalto University has expertise, e.g., in power electronics for ac drives, dc–dc converters, modeling of converters, filtering of EMI, power factor correction, and distributed power systems.

Ricky Chan received his Ph.D. in Electrical Engineering from Purdue University, U.S.A in 2009.

Following graduation, he has held various positions in R&D and product development with A*STAR, Rolls – Royce Singapore, and ABB. Ricky is now R&D / Technology Manager with ABB Marine & Ports in Helsinki, Finland.

Sami Kanerva received the D.Sc. degree from Helsinki University of Technology in 2005.

Since graduation, he has intensively worked on technology concepts for renewable energy and marine technology. Sami has held several R&D positions and gained previous experience on electric machines, drives, wind turbines and power systems. Currently, he is a Senior Principal Engineer in the technology development at ABB Marine & Ports. He has conducted development of marine fuel cell systems at ABB since 2017.